An overview of Marine Vibrator data processing and the value of sweep estimation

Arash JafarGandomi[1], Robert Telling[1], Robert Laws[2], Sergio Grion[1], Aparajita Nath[1] and Tiexing Wang[1],
[1] Shearwater GeoServices, [2] Havakustik Ltd.

Abstract

Marine seismic vibrators are considered serious contenders to air-gun arrays. While the reduced environmental impact is highly attractive, an additional driver is the ability to control the characteristics of the released energy precisely. Here we review how to acquire and process seismic data with marine vibrators while employing a frequency-dependent spatial sampling with and without crossline source-gradient sweeps up to 150Hz, extending previous works which were up to 50Hz. Furthermore, we overview the key processing challenges associated with this advanced acquisition design. In particular, we detail the estimation of the source signature using a joint inversion approach, for accurate and effective sweep deconvolution.

Introduction

The high-precision signal control that marine vibrators achieve allows for novel strategies in survey design (Laws *et al.*, 2019). An array of projector units will typically entail several units deployed at different depths, each active in a frequency band that maximizes constructive source ghost interference and minimizes rough-sea effects (JafarGandomi *et al.*, 2020). The use of diverse frequency bands and phase encoding allows for continuously active simultaneous sources. The low frequencies will typically have longer sweep lengths than higher frequencies. We examine actuating low-band vibrators less frequently (every 10s) than the high-band vibrators (every 5s), which provides denser spatial sampling for higher frequencies needed to tackle spatial aliasing. It is also possible to operate a pair of projector units alternatively in phase and anti-phase, thereby generating both omni-directional and gradient sweeps. Gradient sweeps produce complementary information to omni-directional sweeps, and when generated in the cross-line direction they are a proxy for generating the cross-line gradient of the wavefield. Laws *et al.* (2019) describe the significant benefit of combining gradient and omni-directional sweeps to interpolate recorded data between neighbouring source-lines. Figure 1 shows time slices from modelled common-receiver gathers for the omni (Figure 1a) and gradient sweeps (Figure 1b). Strong wavefield energy in the x-direction (normal to sail line direction) is obvious in the time slice of the gradient sweep data.
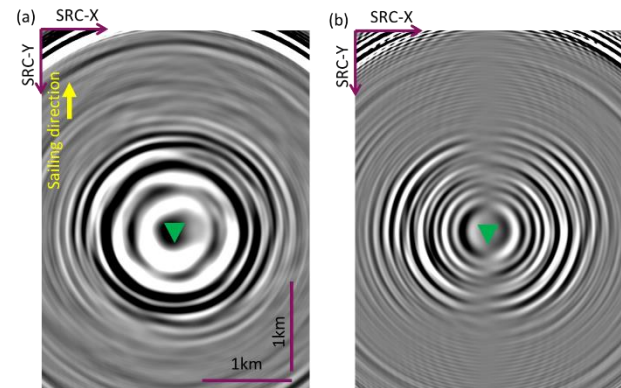
Figure 1 - *A time-slice from a modelled marine vibrator common-receiver gather after processing, for (a) omni sweeps and (b) gradient sweeps. Green triangle indicates receiver location.*

The key processing steps are the estimation of the sweep signature, the compensation of source motion and rough sea effects, sweep deconvolution and de-ghosting, and the de-blending of signals from several phase-encoded sources. The presence of stronger direct arrival and short-period multiples in shallow water bring noticeable challenges compared to the deep-water setups. We employ a sparse inversion approach to reshape marine vibrator data to impulsive-source data in the frequency range 3-150Hz. This allows for subsequent processing to be carried out using conventional techniques. The interplay between the various acquisition effects calls for a joint inversion with sparsity constraints. We have tried different approaches, among which the orthogonal matching pursuit algorithm seems to provide the most promising results.

A key difference between marine and land vibrators is the absence in the marine case of coupling issues between propagating medium and vibrator. This allows a highly accurate estimation of the sweep signature for the marine vibrator, which consequently allows effective deconvolution of the sweep from the data. This is in contrast to the correlation of the data with the sweep with land vibrator data which is not able to completely remove the source effects from the data. Due to the importance of this step, in the following section we describe an approach for the sweep estimation based on a joint inversion of near-field measurements and then an overview of the subsequent processing steps.
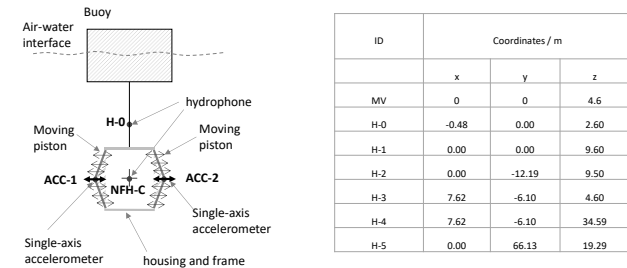
Estimation of the sweep signature

The electrical input signal used to drive the vibrator gives a reasonable 'pilot' signature but it does not generally represent the wavefield emitted in the water to a high enough degree of accuracy. Near-field hydrophone (NFH) measurements provide a means to estimate this wavefield and take account of any transducer-related distortions, complexity in the radiation pattern and interaction with nearby interfaces, as is done for conventional airgun-based sources. However, uniquely for a vibrator source, we are also able to measure the acceleration of the vibrating surface, from which the volume displacement and radiated waveform can be inferred. Signature estimation can thus be approached using either of these measurements independently, each relying on certain assumptions and subject to usual measurement errors. We go further and describe a method that combines these measurements to solve optimally for notional source signatures, which can then be used to construct a robust and accurate estimate of the far-field signature of the source.

The basic method of signature estimation for an array of marine vibrators is to solve for a simplified set of notional signatures for each element in the array. These can then be linearly combined and re-ghosted to generate the far-field signature at the desired take-off angle, an approach which is well-documented for airgun arrays (Ziolkowski *et al.*, 1982, Hargreaves *et al.*, 2015) using NFH measurements. This approach is also taken for measurements of the linear acceleration of the driven surfaces. For a source that is small compared to the emitted wavelength, the second derivative of volume displacement is proportional to the radiated acoustic pressure (Elboth *et al.*, 2022, Kinsler *et al.*, 2000) and for a fixed and known radiator area this then becomes proportional to the linear acceleration measured at the radiator surface.

An advantage of the acceleration measurements is that it is not necessary to take into account cross-talk of arrivals from other vibrators nor ghosting at the sea-surface when deriving the notional sources because the accelerometers measure the volume acceleration, which is directly related to the notionall source. However, there may be non-radiating vibration noise present and also contributions to the radiated wavefield that originate from other parts of the body of the vibrator may be missed. In contrast, the near-field pressure measurement will record the superposed wavefield emitted from each active source element, including interactions and reflections from nearby interfaces. It is therefore a more complex but more complete measurement, potentially subjected to a higher level of environmental noise. Given that both approaches have limitations and the measurements subject to noise, we explore combining them in a joint, least-squares inversion to offer a more robust estimate of the complete source signature in the far field, with the detail of the scheme described in Telling *et al.* (2023).

For testing purposes signatures were estimated for a marine vibrator suspended at 4.6 m depth at the Seneca Lake test facility. The output signal was a linear up-sweep spanning approximately the bandwidth 3-150 Hz and of duration 5s. Data were acquired using the attached NFH and accelerometers together with six external hydrophones with the geometry given in Figure 2. Sensor readings were converted to physical units using nominal sensitivities. Supplying different sensor combinations to the inversion problem, we solved for the notional signatures via a least squares conjugate-gradient iterative solver. We then forward-modelled (propagated) the notional signatures to the positions of the external hydrophones to compare against the ground truth measurements recorded at those hydrophones.


ID	Coordinates / m		
	x	y	z
MV	0	0	4.6
H-0	-0.48	0.00	2.60
H-1	0.00	0.00	9.60
H-2	0.00	-12.19	9.50
H-3	7.62	-6.10	4.60
H-4	7.62	-6.10	34.59
H-5	0.00	66.13	19.29

Figure 2 - *Schematic single vibrator unit and near-field sensors (left) and coordinates of external hydrophones positioned in the lake test facility (right)*

We used the predicted traces at each hydrophone to deconvolve the observed traces to generate the zero-phase wavelet shown in Figure 3 for a full sensor suite together with a quantitative assessment in Figure 4 of the residual for the four different sensor configurations: 1) central NFH, 2) radiator accelerometers, 3) joint inversion using the central NFH and radiator accelerometers, 4) joint inversion with central NFH and hydrophone H0 and the radiator accelerometers. The deconvolution results for hydrophones H0, H1, H2, H5 showed no strong artefacts and alignment within ± 1ms. For H3 the timing error was closer to 2ms, and there was some asymmetry in the resulting wavelet. H3 is the hydrophone positioned at the same depth as the vibrator, and the error here could be related to scattering from the adjacent barge structure.
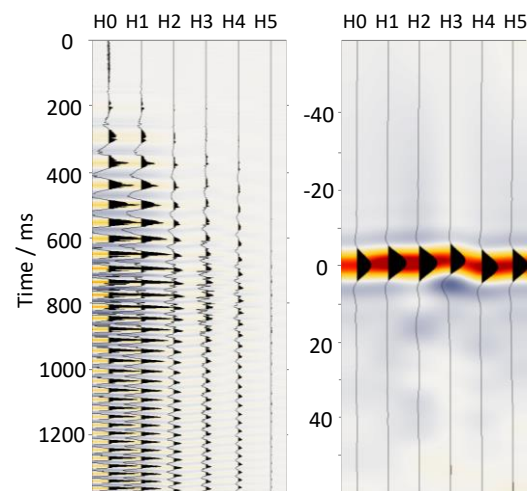
Figure 3 - *Snippet of observed 5s sweep recorded by H0-H5 showing the first 1.4 s (left) and after deconvolution (right) using the forward modelled trace.*

The maximum residual errors over the swept bandwidth lay within ± 5 dB but were more typically ± 3 dB. Configuration 1 showed the largest residual error, and this was significantly reduced in the case of the two configurations 3 and 4 corresponding to joint inversion of hydrophone and accelerometer data. Configuration 2, using just accelerometers, resulted in a lower residual than the case of a single hydrophone.
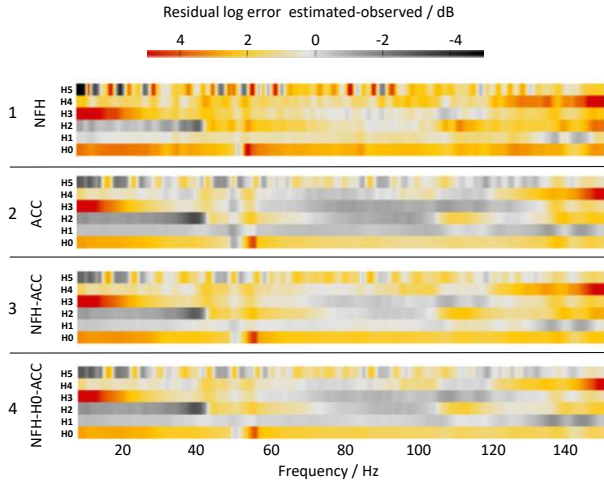
Figure 4 - *Residual error between predicted and observed log power spectra as a function of frequency at external hydrophones.*

This benchmarking configuration was inherently near field, meaning that approximations in the model used for deriving far-field signatures will be exposed more acutely. Interactions including reflections and scattering from the nearby buoy and barge as well as reflections from the lakebed were neglected in the estimation method. Nevertheless, the closeness between predicted and observed traces and resulting deconvolution gives encouragement that the method has a sound basis for robust signature estimation.

Processing of synthetic data

In this section we use synthetic data to illustrate marine vibrator data processing. We consider synthetic data using a modified SEAM phase 1 model for an ocean bottom node acquisition scenario. The marine vibrator source array consists of three source units, one low-band (3-25Hz) deployed at 15m depth, and two high-band (25-150Hz) deployed at 5m depth, emitting 10s and 5s sweeps, respectively. With a vessel speed of 2.5m/s, the continuous emission leads to equivalent nominal sweep-point spacing of 12.5m for the high-band and 25m for the low-band sweeps. The crossline spacing between the neighboring source-lines is 50m.

To facilitate de-blending, carefully designed phase modulation sequences are applied to the low- and high-band sweeps. Phase modulation shifts signal content to pre-determined wavenumbers, therefore facilitating deblending (Laws *et al.*, 2019). Since the marine vibrators operate continuously, without separate sweeping and listening times, signals from adjacent sweeps overlap and require deblending.
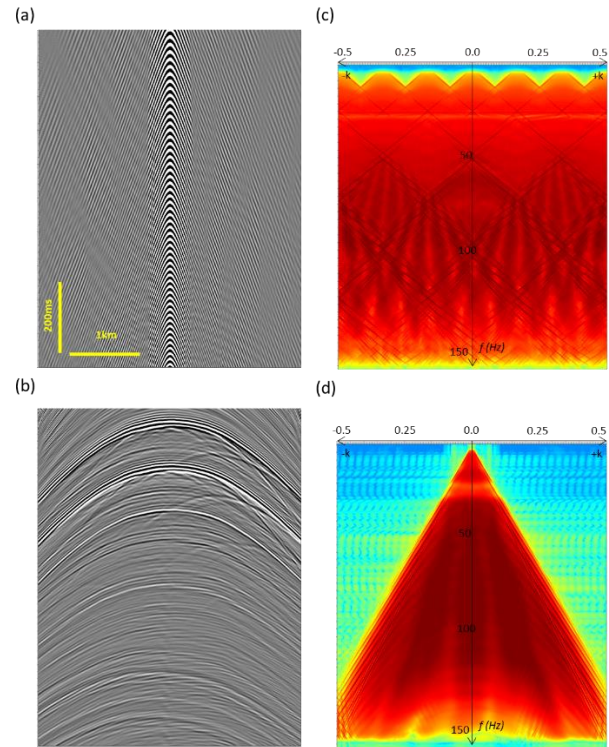
Figure 5 – (a,c) *Raw synthesized marine vibrator data using an array of one high-band unit and one low-band unit including phase encoding, source ghost and source motion and b,d) data after full processing. Wavenumbers in (c) are normalized, scaled by the trace spacing 12.5m and for (d) 6.25m.*

The periodical phase sequence chosen for subsequent sweeps is 0º, 120º, 120º (Nath *et al.*, 2022). As the low-band sweeps are actuated at every other sweep-start location, their corresponding phase modulation is also 0º, 120º, 120º. This sequence allows the optimal separation in wavenumber space of 3 signals: it is expected that with the 5s long sweep time no more than 3 adjacent sweeps will give rise to significant blending. It also ensures that when low-band and high-band sweeps overlap, they have the same phase modulation.

The aim of the processing step illustrated here is to reconstruct impulsive, redatumed, source-ghost free receiver records with the desired shot point grid from the simulated marine vibrator data acquired in continuous mode, with all vibrators simultaneously sweeping. There are several acquisition-related effects that require compensation in order to meet this objective. The reconstruction algorithm needs to perform:

- Source motion compensation
- Sweep deconvolution and phase demodulation
- Deblending
- Source de-ghosting and redatuming

The challenge of compensating for these effects is compounded by the complexity of the marine vibrator array, consisting of several projector units operating at different depths, within differing frequency bands and with specific sweeps and phase modulation. Since modelling of these effects is feasible (see for example JafarGandomi and Grion 2021), these challenges can be formulated as inverse problems.

One fundamental choice in facing these challenges is whether to tackle them one at a time by separate inversions, or jointly. We favor the joint approach discussed in Laws *et al.*, (2019), for the following reason. Deblending is an under-determined problem where signals overlap, and its solution requires sparsity constraints, and joint inversion leads to the sparsest representation of the impulsive source data in the model space.

Another factor in favor of joint inversion is that each of the effects to be compensated depends on source coordinates, frequency and source-side take-off angles, and therefore they can all be observed in the same domain, the common receiver gather, and can be modelled in the same transform domain of this gather.

The joint inversion algorithm takes as input the marine vibrator data recorded by each ocean bottom node, the vibrator array configuration and its navigation information. For illustration purposes, Figure 5 shows an example of data before and after reconstruction of the corresponding impulsive source signal, with an additional intermediate step where only sweep deconvolution and phase demodulation are applied.

Figure 5a shows the synthesized data as input to the processing flow. The corresponding f-k spectrum in Figure 5b shows 6 signal cones. These result from the complex setup of the array, the fact that the low-band sweeps are not initiated at every sweep-start location, and the phase modulation used. Figure 5b presents the final processed data after source-motion correction, source de-ghosting, re-datuming, and reconstruction to a 6.25m grid in two orthogonal directions. The f-k spectrum in Figure 5d now shows the expected single signal cone delimited by the dispersion relation, typical of a marine ocean-bottom common receiver gather.

Conclusions

Marine vibrators offer a range of exciting survey design and data processing opportunities. Its sound emissions are expected to be environmentally friendlier and more efficient due to its continuous operation at lower peak levels than air gun arrays. Several units can be simultaneously active, covering different frequency bands with different spatial samplings. Employing phase encoding provides a great opportunity for the effective de-blending of simultaneous sources at the processing stage. We emphasize that accurate estimation of the sweep signature using near source measurements is essential for successful deconvolution of the sweep and the subsequent processing steps. We show that using sparse inversion it is possible to remove all acquisition effects, however, the inclusion of these effects in FWI modelling also appears attractive and should be explored further.

References

ELBOTH, T.; AUNE, H.; MELBØ, A. H.; LAWS, R. 2022. A 4D Ready Marine Vibrator. 83rd EAGE Annual Conference and Exhibition 2022 1-5.

HARGREAVES, N.; GRION, S.; TELLING, R. 2015. Estimation of air-gun array signatures from near-gun measurements – least-squares inversion, bubble motion and error analysis. 85th SEG Meeting, Expanded Abstracts, 149-153.

JAFARGANDOMI, A.; GRION, S.; 2021, Modelling of marine vibrator data, 82nd EAGE Annual Conference and Exhibition 2021.

JAFARGANDOMI, A.; GRION, S.; HOLLAND, S. 2021. marine vibrator array design: an obs example, in first International Meeting for Applied Geoscience & Energy (71-75).

KINSLER, L. E.; FREY, A.R.; COPPENS, A. B; SANDERS, J. V. 2000 Fundamentals of Acoustics, 4th Edition, John Wiley and Sons Inc.

LAWS, R.M.; HALLIDAY, D.; HOPPERSTAD, J-F.; GEREZ, D.; SUPAWALA, M.; ÖZBEK, A.; MURRAY, T.; KRAGH, E. 2019. Marine vibrators: the new phase of seismic exploration. Geophysical Prospecting. 67,1443-1471.

NATH, A., JAFARGANDOMI, A.; GRION, S.; 2022. Enhanced Source Separation for Phase-Sequenced Simultaneous Source Marine Vibrator Data, 83rd EAGE Annual Conference and Exhibition.

TELLING, R.H.; JAFARGANDOMI, A.; LAWS, R.M.; GRION, S. 2023 Estimating the signature of a marine vibrator by joint inversion of hydrophone and accelerometer measurements, 84th EAGE Annual Conference and Exhibition.

ZIOLKOWSKI, A.; PARKES, G.; HATTON, L.; HAUGLAND T. 1982. The signature of an air gun array: Computation from near-field measurements including interactions. Geophysics, 47, 1413-1421.